Journal of Applied Research and Technology

www.jart.icat.unam.mx

Journal of Applied Research and Technology 21 (2023) 808-824

Original

Curcumin dye adsorption in aqueous solution by carbon-based date palm seed: Preparation, characterization, and isotherm adsorption

A.B.D. Nandiyanto* • R. Ragadhita • M. Fiandini • R. Maryanti

Universitas Pendidikan Indonesia, Jl. Dr. Setiabudi No. 229 Bandung, Indonesia

Received 04 21 2022; accepted 03 23 2023
Available 10 31 2023

Abstract: This work examined the isotherm adsorption of carbon microparticles from date palm seeds. To produce carbon microparticles, date palm seeds were carbonized at 250°C for three hours, followed by a saw-milling and sieving procedure. To support the analysis, several characterizations were performed, including physicochemical properties and morphology characterizations (by microscope), chemical composition analysis (Fourier transform infrared), and adsorption examination (by adsorbing curcumin in aqueous solution, compared to 10 adsorption isotherm models). To confirm the phenomena during the adsorption of curcumin, three sizes of carbon microparticles were employed (i.e., 500, 250, and 100 µm). All adsorption processes were done in the batch reactor at room temperature and pressure. The results showed that adsorption efficiency correlated to the size of the carbon microparticles as adsorbent, in which the efficiencies of carbon microparticles with sizes of 500, 250, and 100 µm were 34.10, 49.70, and 53.44%, respectively. The isotherm adsorption showed the carbon microparticles followed Langmuir > Dubinin-Radushkevich > Jovanovic > Freundlich > Halsey models. The analysis showed that the adsorption was done in a normal, spontaneous, and favorable process, confirming monolayer and multilayer formation on heterogeneous surfaces. The process follows cooperative adsorption with chemical and physical interactions. The paper includes information on date palm seed adsorbents produced for water treatment and their prospective use as adsorbents, which can be used for solving issues in the Sustainable Development Goals (SDGs).

Keywords: Adsorption, carbon, curcumin, date palm seed, isotherm adsorption, particles

*Corresponding author.
E-mail address: nandiyanto@upi.edu (A.B.D. Nandiyanto).
Peer Review under the responsibility of Universidad Nacional Autónoma de México.

1. Introduction

The utilization of carbon as a material in significant applications is widely documented. Carbon is one of the most often used materials (Awan et al., 2017a; Awan et al., 2017b; Awan et al., 2019; Efiyanti et al., 2020; Sambudi et al., 2022; Nandiyanto et al., 2023; N'diaye, 2023). It is because of how well it works in the adsorption process (Anshar et al., 2016). Many techniques have been used to produce carbon for adsorbent, but the challenge in the utilization of carbon particles is to get an economical, sustainable, and environmentally friendly resource and adsorbent product. The most effective ones include converting biomass and agricultural waste (see Table 1) (Fiandini et al., 2020; Nandiyanto, Girsang, et al., 2020; Ragadhita et al., 2019; Nandiyanto, 2020; Nandiyanto, Arinalhaq et al., 2020; Nandiyanto et al., 2021; Nandiyanto, Maryanti et al., 2020).

This study demonstrated the production of carbon-based adsorbents from date palm seed waste. Although a variety of raw materials have been considered as prospective possibilities for carbon preparation, there has not yet been any research on date palm seeds as an effective low-cost carbon preparation. Date palm seed is one of the most common agricultural wastes with no commercial value. Date palm seeds are typically cultivated in the Middle East, and they are hardly found in Southeast Asia, such as Indonesia. However, since dates are employed in Muslim religious rites, particularly during the holy month of Ramadan, dates cannot be separated from Indonesian culture. Date seed waste is therefore prevalent in Indonesia during the holy month of Ramadan (date palm seeds make up roughly 11–18% of the weight of date fruit), although date seeds are still regarded as waste from the production of date-based goods). Large quantities of date palm seed thus accumulate as waste with no further use. Recognizing the process for reusing waste from date palm seed is important since it acts as a superior carbon source. Date palm seeds have high lignocellulosic content (Chang et al., 2020). Date seed contains 42% cellulose, 25% hemicellulose, and 11% lignin (Bouchelta et al., 2008). Although research on the utilization of date palms has been reported (Nabili et al., 2016; Nayl et al., 2017), analysis of the phenomena happening during the adsorption using carbon particles from date palms is typically nonexistent. This study used curcumin (as a model of dye) from aqueous solutions, which were done in the batch process under room temperature and pressure. To support the adsorption performance of date palm seeds, this study also investigated and evaluated the adsorption results by comparing them with current isotherm adsorption models. Although other research (as shown in Table 1) has established that carbon-based materials from agricultural waste sources have the best fit with the Freundlich adsorption isotherm model, this study evaluated and tested for 10 types of isotherm models (i.e., Langmuir, Freundlich, Temkin, Dubinin-Radushkevich, Fowler-Guggenheim, Hill-Deboer, Jovanovic, Harkin-Jura, Flory-Huggins, and Halsey) to make sure the phenomenon was occurring. To clarify the phenomena, we explored and assessed the suitability of adsorption isotherms with different sizes (i.e., 500, 250, and 100 µm).

2. Isotherm adsorption theory

Adsorption isotherm models such as Langmuir, Freundlich, Temkin, Dubinin-Radushkevich, Fowler-Guggenheim, Hill-Deboer, Jovanovic, Harkin-Jura, Flory-Huggins, and Halsey are used to evaluate the phenomenon during the adsorption process. When adsorption occurs in a monolayer, multilayer, or cooperative manner, this is a possible phenomenon of standard adsorption processes. Figure 1 depicts the phenomenon of the monolayer, multilayer, and cooperative adsorption processes. An explanation of the adsorption isotherm model is provided in detail below (Ragadhita & Nandiyanto, 2021).

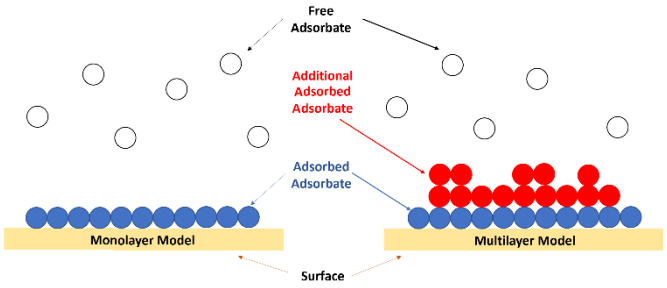

Figure 1. Illustration of the monolayer, multilayer, and cooperative adsorption process (Ragadhita & Nandiyanto, 2021).

2.1. Langmuir model

The Langmuir equation assumes that adsorption occurs on the specific surface of a homogeneous adsorbent. In addition, the Langmuir isotherm only forms a single layer when maximum adsorption, each atom is only adsorbed at the location on the adsorbent surface, and each part of the surface can only contain one molecule or atom. The Langmuir adsorption isotherm is written in Eq. (1) and (2).

$$\frac{1}{Q_e} = \frac{1}{Q_{max} K_L} \frac{1}{C_e} + \frac{1}{Q_{max}} \quad (1)$$

$$R_L = \frac{1}{1 + K_L C_e} \quad (2)$$

Where K_L is the Langmuir adsorption constant, Q_{max} is the adsorption capacity of the monolayer (mg/g), and R_L is the separation factor. Table 2 shows the meaning of the R_L parameter.

Table 1. Recent studies on the utilization of agricultural waste-based adsorbents.

Source of Agricultural Wastes	Adsorbent Type	Adsorbed Molecule Model	Results	Ref.
Pineapple peel	Carbon Microparticles	Curcumin Solution	The adsorption profile matches the Freundlich model which indicates that on the heterogeneous surface of the adsorbent, multilayer formation occurs. The interaction between the adsorbed molecules is of the type of physisorption (Van der Waals). The presence of multilayer formation is not accompanied by cooperative interactions between the adsorbed molecules because the adsorbent surface is porous.	(Nandiyanto, Girsang et al., 2020)
Rice Husk	Silica	Curcumin Solution	The adsorption equilibrium data matched the Freundlich model. Freundlich isotherm informs that the surface is heterogeneous and multilayer formation occurs. The surface of the adsorbent also contains mesoporous pores, so the adsorption rate is low.	(Ragadhita et al., 2019)
Rice Husk	Porous Activated Carbon	Curcumin Solution	The experimental results show that the adsorption process follows the Freundlich model which informs the formation of multilayers on a uniform surface. The use of porous structures in the adsorption process allows for greater adsorbate diffusion into the surface site and improved adsorption efficiency.	(Fiandini et al., 2020)
Pumpkin (Cucurbita maxima) Seeds	Carbon	Curcumin Solution	The models demonstrated that adsorbates interact with the carbon in multilayers via physical processes. The inorganic content of pumpkin seeds allows for the formation of carbon with porosities, resulting in more adsorption sites. Adsorbed molecules attract and bind to other free molecules. Adsorption occurs on energetically distinct sites in an endothermic process.	(Nandiyanto, 2020)
Soursop (AnnonaMuricata L.) Peel	Carbon Microparticle	Curcumin Solution	In the adsorption process the formation of a multilayer with adsorbate-adsorbate interaction is physical interaction (physisorption). Adsorption occurs energetically at various locations via endothermic processes. The calculated Gibbs free energy for all models is negative, indicating that the adsorption process occurs spontaneously.	(Nandiyanto, Arinalhaq et al., 2020)
Pumpkin (Cucurbita maxima) Seeds	Carbon Microparticle	Curcumin Solution	Adsorption with smaller particles has a direct impact on increasing adsorption capacity due to the presence of a larger surface area, a greater number of adsorption sites, and additional cooperative adsorption, i.e., adsorbate-adsorbate interaction.	(Nandiyanto et al., 2021)
Red Dragon Fruit (Hylocereus undatus) Peel	Carbon Microparticles	Curcumin Solution	The results of the analysis revealed that multilayer adsorption occurs for all sizes in the micrometer range and that the process involves physical interactions between adsorbate and adsorbent surfaces. The presence of multilayers is due to the possibility of porous structures in carbon microparticles.	(Nandiyanto, Maryanti, et al., 2020)

Table 2. The meaning of the R_L parameter.

Condition	Explanation
$R_L > 1$	Unfavorable adsorption because desorption occurs
$R_L = 1$	Linear adsorption process that does not depend on the concentration
$R_L = 0$	Irreversible adsorption process because the adsorbate cannot diffuse (usually occurs in chemisorption)
$0 < R_L < 1$	Favorable adsorption because no desorption occurs

2.2. Freundlich model

Freundlich isotherm assumes that the adsorbent has a heterogeneous surface, and each molecule has a different adsorption potential. This equation is the most used. The Freundlich equation also shows the adsorption process, which is either reversible or irreversible, and still not forbidden to form an adsorption process that is a monolayer. The isotherm equation is expressed by Eq. (3).

$$log\ log\ Q_e = logk_f + \frac{1}{n} log\ log\ C_e \quad (3)$$

Where k_f is the Freundlich constant that estimates the adsorption capacity, C_e is the adsorbate concentration at equilibrium (mg/L), n is the degree of linearity, and $1/n$ assumes the adsorption strength. n and $1/n$ parameters have the meaning as shown in Table 3.

Table 3. The meaning of the n and $1/n$ parameters.

Condition	Explanation
$n < 1$	Characteristic of the adsorption process with the chemisorption process
$n = 1$	Characteristic of a linear adsorption process where there is a partition between two phases that is independent of concentration
$n > 1$	Characteristic of the adsorption process with the physisorption process
$1/n < 1$	Characteristic of the normal adsorption process
$1/n > 1$	Characteristic of the cooperative adsorption process
$1 < 1/n < 0$	Characteristic of a favorable adsorption process because there is no desorption process
$0 < 1/n < 1$	Characteristic of the adsorption process that occurs on heterogeneous surfaces (a $1/n$ value close to 0 indicates that the adsorbent surface is increasingly heterogeneous).

2.3. Temkin model

This type of isotherm contains an explicit factor related to the adsorbent-adsorbate interaction. By ignoring very low or high concentration values, this model assumes that the energy or heat of adsorption (a function of temperature) of all molecules in the layer will decrease linearly with increased coverage caused by adsorbent-adsorbate interaction, due to adsorbate-adsorbate repulsion and adsorbate adsorption uniformly distributed between layers. The Temkin isotherm equation is written in Eq. (4).

$$q_e = \beta_T(lnC_e) + (\beta_T lnA_T) \quad (4)$$

Where A_T is the equilibrium constant of the Temkin isotherm model and β_T is the Temkin isotherm. β_T parameter is explained in Table 4.

Table 4. The meaning of the β_T parameter.

Condition	Explanation
$\beta_T < 8$ kJ/mol	Physical adsorption
$\beta_T > 8$ kJ/mol	Chemical adsorption

2.4. Dubinin-Radushkevich model

The Dubinin-Radushkevich isotherm is generally applied to describe the adsorption mechanism with the distribution of Gaussian energy on a heterogeneous surface, The Dubinin-Radushkevich isotherm model predicts that the adsorption process follows a pore-filling mechanism. This model assumes that the adsorption has a multilayer character, involves van der Waals forces, and applies to the adsorption process physics. The Dubinin-Radushkevich isotherm equation is presented in Eq. (5).

$$lnq_e = lnq_s - \beta\varepsilon^2 \quad (5)$$

Where q_s is the theoretical saturation capacity (mg/g), is the Dubinin-Radushkevich isotherm constant which is correlated with the average free adsorption energy per mole of adsorbate, and $\boldsymbol{\varepsilon}$ is the Polanyi potential associated with equilibrium conditions. The Polanyi potential and the calculation of the adsorption energy are expressed by Eq. (6) and (7).

$$\varepsilon = RT\ ln\ ln\left[1 + \frac{1}{C_e}\right] \quad (6)$$

$$E = \frac{1}{\sqrt{2\beta}} \quad (7)$$

Where E is the adsorption energy which has the meanings shown in Table 5.

Table 5. The meaning of the *E* parameter.

Condition	Explanation
$E < 8$ kJ/mol	Physical adsorption
$E > 8$ kJ/mol	Chemical adsorption

2.5. Fowler-Guggenheim model

The Fowler-Guggenheim isotherm explains how adsorbed molecules interact with one another. Eq. (8) expresses the Fowler-Guggenheim isotherm.

$$K_{FG}C_e = \frac{\theta}{1-\theta} exp(\frac{2.\theta.W}{RT}) \quad (8)$$

Where K_{FG} is the Fowler-Guggenheim equilibrium constant (L/mg), and W is the interaction energy between the adsorbed molecules (kJ/mol). Table 6 summarizes the meaning of the W parameter.

Table 6. The meaning of the *W* parameter.

Condition	Explanation
$W > 0$ kJ/mol	The attractive force between the adsorbed molecules and the process is exothermic
$W < 0$ kJ/mol	The repulsion between the adsorbed molecules and the process is endothermic
$W = 0$ kJ /mol	No interaction between the adsorbed molecules

2.6. Hill-Deboer model

The Hill-Deboer isotherm model describes a situation in which there is both mobile adsorption and lateral interaction between adsorbed molecules (Rajabi et al., 2023; Jeyavishnu & Alagesan, 2020). The equation for the Hill-de Boer isotherm is expressed by Eq. (9).

$$K_1.C_e = \frac{\theta}{1-\theta} exp(\frac{\theta}{1-\theta} - \frac{K_2\theta}{RT}) \quad (9)$$

Where K_1 is the Hill-de Boer constant (L/mg), and K_2 is the energetic constant of the adsorbed molecular interaction. Table 7 shows the meaning of the K_2 parameter.

Table 7. The meaning of the K_2 parameter.

Condition	Explanation
$K_2 > 0$ kJ/mol	The attractive force between the adsorbed molecules and the process is exothermic
$K_2 < 0$ kJ/mol	The repulsion between the adsorbed molecules and the process is endothermic
$K_2 = 0$ kJ/mol	No interaction between the adsorbed molecules

2.7. Jovanovic model

The Jovanovic model is based on the same assumptions in the Langmuir model, but it also considers the possibility of mechanical contact between the adsorbate and adsorbent. The linear equation of the Jovanovic isotherm is shown by Eq. (10).

$$lnQ_e = lnQ_{max} - K_jC_e \quad (10)$$

Where Q_e is the amount of adsorbate in the adsorbent at equilibrium (mg/g), Q_{max} is the maximum adsorption of the adsorbate, and K_J is the Jovanovic constant.

2.8. Harkin-Jura model

The Harkin-Jura isotherm model predicts multilayer adsorption on the surface of adsorbents with heterogeneous pore distribution. The equation of this model is expressed by Eq. (11).

$$\frac{1}{q_e^2} = \frac{B_{HJ}}{A_{HJ}} - \left(\frac{1}{A}\right) logC_e \quad (11)$$

where B_{HJ} is related to the specific surface area of the adsorbent and A_{HJ} is the Harkin-Jura isotherm constant.

2.9. Flory-Huggins model

The Flory-Huggins isotherm considers the surface coverage of the adsorbate on the adsorbent and assumes that the adsorption process occurs spontaneously. Eq. (12) represents the Flory-Huggins isotherm.

$$log\frac{\theta}{C_e} = logK_{FH} + n\ log\ log\ (1-\theta) \quad (12)$$

Where $\theta = (1 - \frac{C_e}{C_o})$ which indicates the degree of surface coverage, K_{FH} is the Flory-Huggins isotherm constant, and n_{FH} is the amount of adsorbate occupying the adsorption site. To calculate the

Gibbs free energy ($\Delta G°$) of adsorption that occurs spontaneously, the value of $\Delta G°$ can be calculated from the equilibrium constant (K_{FH}) which is shown by Eq. (13).

$$\Delta G° = -RTlnK_{FH} \quad (13)$$

The negative value of $\Delta G°$ indicates that the adsorption process is spontaneous and depends on temperature.

2.10. Halsey model

The Halsey isotherm evaluates adsorption with multilayer characteristics. The equation of the Halsey isotherm is shown by Eq. (14).

$$Q_e = \frac{1}{n_H} lnK_H - \left(\frac{1}{n_H}\right) lnC_e \quad (14)$$

Table 8. Adsorption isotherms fitting data, calculation, and their parameters.

Isotherm Model	Linear Equation	Plotting		Parameters
		x-Axis	y-Axis	
Langmuir	$\frac{1}{Qe} = \frac{1}{QmaxK_L}\frac{1}{Ce} + \frac{1}{Qmax}$	$\frac{1}{C_e}$	$\frac{1}{Q_e}$	• $\frac{1}{Q_{max}} = intercept$ • $K_L = \frac{1}{Q_{max} \times slope}$
Freundlich	$ln\ ln\ Q_e = ln\ k_f + \frac{1}{n}\ ln\ ln\ C_e$	lnC_e	lnQ_e	• $lnK_F = intercept$ • $\frac{1}{n} = slope$
Temkin	$q_e = B_T\ ln\ ln\ A_T + B_T\ ln\ ln\ Ce$	lnC_e	Q_e	• $B = slope$ • $B_T lnA_T = intercept$ • $B_T = \frac{RT}{B}$
Dubinin-Radushkevich	$ln\ ln\ q_e = ln\ ln\ q_s - (\beta\varepsilon^2)$	ε^2	lnQ_e	• $\beta = K_{DR} = slope$ • $E = \frac{1}{\sqrt{2 \times K_{DR}}}$
Flory Huggins	$log\frac{\theta}{C_e} = logK_{FH} + nlog(1-\theta)$	$log\ log\left(\frac{\theta}{C_0}\right)$	$log(1-\theta)$	• $n_{FH} = slope$ • $k_{FH} = intercept$ • $\Delta G^{\circ} = RTln(k_{FH})$ $\theta = 1 - (\frac{C_e}{C_0})$
Fowler-Guggenheim	$ln\left(\frac{C_e(1-\theta)}{\theta}\right) - \frac{\theta}{1-\theta} = -lnK_{FG} + \frac{2W\theta}{RT}$	θ	$ln\left[\frac{C_e(1-\theta)}{\theta}\right]$	• $W = slope$ • $-lnK_{FG} = intercept$ • $\alpha\ (slope) = \frac{2W\theta}{RT}$ $\theta = 1 - (\frac{C_e}{C_0})$
Hill-Deboer	$ln\left[\frac{C_e(1-\theta)}{\theta}\right] - \frac{\theta}{1-\theta} = -lnK_1 - \frac{K_2\theta}{RT}$	θ	$ln\left[\frac{C_e(1-\theta)}{\theta}\right] - \frac{\theta}{1-\theta}$	• $-lnk_1 = intercept$ • $\alpha\ (slope) = \frac{k_2\theta}{RT}$ • $\theta = 1 - (\frac{C_e}{C_0})$
Jovanovic	$lnq_e = lnq_{max} - K_J C_e$	C_e	lnQ_e	• $K_J = slope$ • $lnq_{max} = intercept$
Harkin-Jura	$\frac{1}{q_e^2} = \frac{B}{A} - \left(\frac{1}{A}\right) logC_e$	$logC_e$	$\frac{1}{q_e^2}$	• $A_H = \frac{1}{Slope}$ • $\frac{B_H}{A_H} = intercept$
Halsey	$lnQ_e = \frac{1}{n_H} lnK_H - \frac{1}{n} lnC_e$	lnC_e	lnQ_e	• $\frac{1}{n} = slope$ • $\frac{1}{n} lnK_H = intercept$

Furthermore, Eq. (15) is used to calculate the amount adsorbed by the unit mass of the adsorbent at equilibrium (Q_e).

$$Q_e = \frac{C_o - C_e}{m} \times V \quad (15)$$

where C_o is the initial concentration (mg/L), C_e is the equilibrium concentration (mg/L), m is the mass of the adsorbent (g), and V is the volume of the adsorbate solution (L).

2.11. Fitting data from models

Adsorption isotherms fitting data, calculation, and their parameters are summarized in Table 8.

3. Materials and methods

3.1. Materials

The materials used in this study were date palm seed, ultrapure water, and curcumin (which were obtained by extracting turmeric from a local market in Bandung, Indonesia).

3.2. Carbon preparation

Date seeds are used to prepare carbon microparticles. Date seeds are washed to remove dirt first and dried. The dried date seeds were then carbonized using an oven at a temperature of 250°C for 3 hours to form carbon particles. After that, the carbon particles formed were ground to obtain fine particles and sieved to determine the specific particle size. The sieve-mesh used was equipped with pans with hole sizes of 500, 250, 100, 74, and 60 µm. For the understanding of the adsorption results, carbon microparticles with sizes of 500, 250, and 100 µm were tested.

3.3. Physicochemical characterization

A digital microscope was used to investigate the particle size and morphology of the raw material (calcium carbonate from chicken bone waste). Fourier transform infrared was used for chemical characterization to analyze elemental structure products (FTIR, FTIR-6600, Jasco Corp., Japan). Then, the analysis in the surface area and porous structure, nitrogen sorption measurement (Brunauer-Emmett-Teller (BET) Nova 4200e; Quantachrome Instruments Corp., US; operated at 77 K) was conducted.

3.4. Batch adsorption experiment

Carbon microparticles (0.05 g) with sizes of 500, 250, and 100 µm were added to the curcumin solution with various initial concentrations (100, 80, 60, 40, and 20 ppm) in a beaker with a capacity of 500 mL. Then, the mixture of the curcumin-carbon solution was shaken using a magnetic stirrer for 120 minutes at room temperature with constant pressure and pH (batch experiment). After the adsorption process was completed, the curcumin solution was filtered to separate the carbon particles using a nylon membrane syringe filter with a pore size of 0.22 µm.

Final concentrations were determined using a UV-VIS apparatus (Model 7205; JENWAY; Cole-Parner; US). The final concentration analysis was carried out by observing the maximum peak of the curve at a wavelength of 280-500 nm. The adsorption results were plotted and normalized. The maximum adsorption peak was calculated using Beer's Law to obtain the concentration of curcumin. The concentration data obtained were plotted and compared with standard adsorption isotherm models: Langmuir, Freundlich, Temkin, Dubinin-Radushkevich, Fowler-Guggenheim, Hill-Deboer, Jovanovic, Harkin-Jura, Flory-Huggins, and Halsey models.

4. Results and discussion

4.1. Physical properties of date palm seed

Figure 2(a) shows digital microscope images, while Figure 2(b) shows a Ferret analysis of carbon particles made from date palm seed. Figure 2(a) demonstrates that the carbon particles are inhomogeneous in size, with a particle size range of 270 – 500 µm. Figure 2(b) depicts the particle size distribution results, which show that most of the carbon particles have sizes ranging from 100 to 300 µm. To give you some perspective, the average particle size of carbon is 260 µm.

Figures 3(a) and (b) were the adsorption/desorption curves to investigate the porosity and surface area of the particles with sizes of 500 and 100 µm, respectively. The characteristics of the adsorbent with a particle size of 500 µm followed Type III isotherm (Figure 3(a)), indicating the existence of micropores. Adsorption does not take place with a single layer of molecules covering the substrate (forming a multilayer). Meanwhile, the adsorbent with a particle size of 100 µm had a BET adsorption type I (Figure 3(b)), implying monolayer molecule adsorption on the substrate. The gaps between the atoms of the carbon microparticles are assumed to be nanometer-sized micropores capable of accepting and trapping molecules via Van der Waals interactions in this case.

Table 9 summarizes the texture characteristics obtained based on the BET and BJH results for carbon microparticles with sizes of 500 and 100 µm. BJH analysis showed both particles had micropores (pore size of about 1.695). Based on Table 9, particle size has an impact on the surface area and pore volume of the adsorbent particles. The smaller size has an impact on the obtainment of a larger surface area and pore volume. For 250-µm carbon microparticles, BET analysis was not performed. However, the characteristics of the 250 µm carbon microparticles can be predicted to have performance between 100 and 500 µm.

In addition, since the pores are in the range of micropore size range (about 1.6 nm; see Table 9), we can conclude that all adsorptions will be done on the outer surface. Molecules must be less than 1 nm to get the deepest pore position.

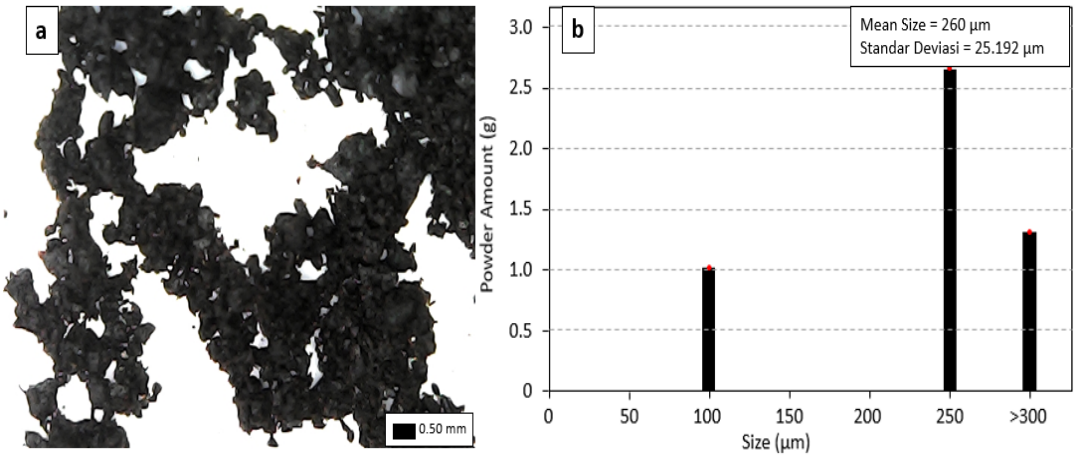

Figure 2. The digital microscope of calcium carbonate (a) and Ferret analysis of particle size (b).

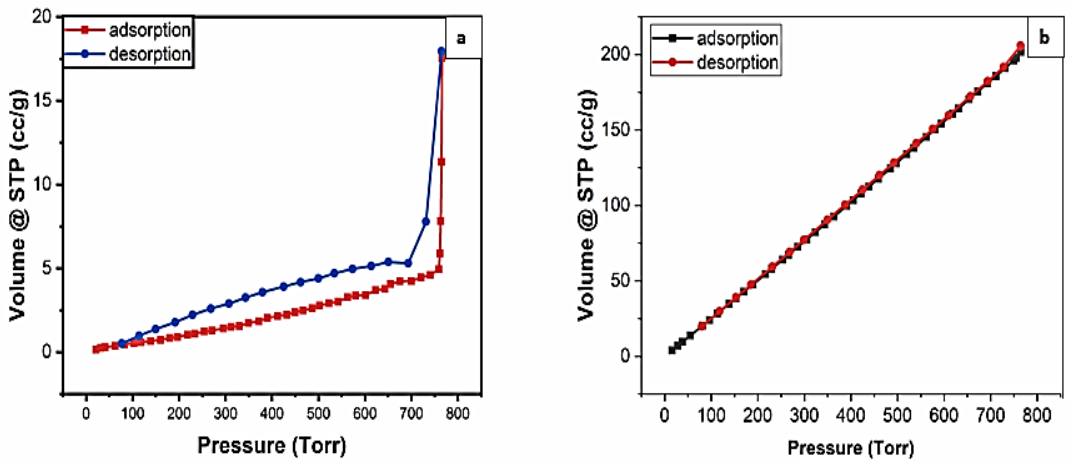

Figure 3. N_2 adsorption-desorption isotherm of carbon microparticle having a size of 500 (a) and 100 (b) µm, respectively.

Table 9. Surface characteristics of carbon microparticles adsorbents with sizes of 500 and 100 µm.

Size of Carbon Microparticles Sample (µm)	BET Type Characteristics	BET Surface Area (m^2/g)	Pore Volume (cm^3/g)	Pore Size (nm)
500	Type-III	5.548	0.026	1.695
100	Type-I	178.604	0.288	1.695

Figure 4 reveals information about the functional groups present in the date palm seed-based carbon and date palm seed. Based on FTIR data, functional groups shift to different frequencies or, in some cases, disappear and appear when date seeds are treated with carbonization. There were broad peaks in the ~3400 - 3100 cm^{-1} region for the date palm seed-based carbon and date palm seed samples which were associated with the O-H stretching vibration of the hydroxyl functional groups. However, in the date seed-based carbon sample, the absorption of functional groups in that area decreased in intensity, indicating the loss of some moisture due to the carbonization process. The peak around 2926.11 - 2856.67 cm^{-1} in both samples indicates the presence of methyl and methylene functional groups associated with asymmetric C-H bands. These absorption bands show contributions from cellulose, hemicellulose, and lignin. The peak in the adsorption area ~1745.65 cm^{-1} in both samples indicated the presence of a carbonyl (C=O) associated with an ester group on the hemicellulose bond or an ester of the ferulic carboxylic group and p-coumaric acid lignin and/or hemicellulose. Vibrations that show aromatic groups such as C=C and C=N are shown in the adsorption around 1627.97 - 1616.40 cm^{-1} in both samples. The aromatic skeleton mode indicated by stretching C=C was indicated by the presence of adsorption around 1446.66 - 1437.02 cm^{-1} in both samples. The peak at 1375.29 cm^{-1} in both samples is caused by cellulose C–H stretching. The adsorption band at ~1242.20 cm^{-1} in both samples is the C-O-H deformation and C-O stretching of the phenolic group. The C–O stretching vibration of cellulose and hemicellulose in both samples is described by the band at 1089.82 - 1057.03 cm^{-1}. The adsorption at 871.85 cm^{-1} in both samples is related to cellulose's C–H rocking vibrations (Nabili et al., 2016). The peaks from the results of the FTIR analysis in detail are also summarized in Table 10.

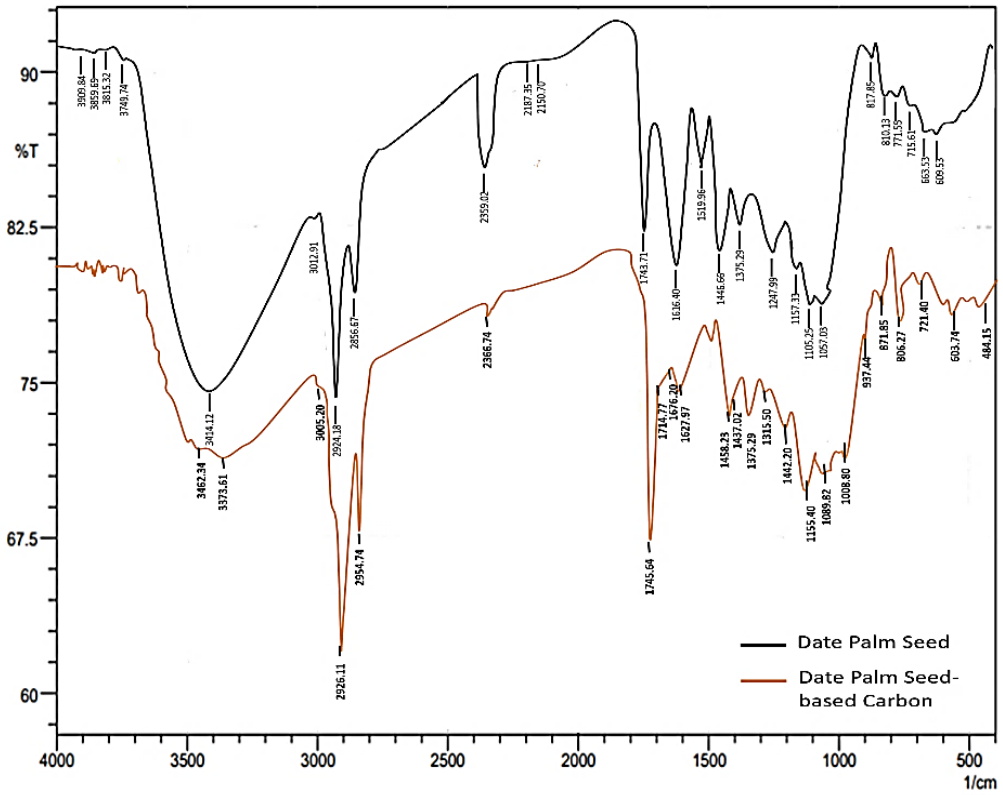

Figure 4. FTIR spectra of date palm seed and date palm seed-based carbon.

Table 10. Summarized of FTIR results of date palm seed.

Wavenumber (cm^{-1})	Band Origin
3373.61	O-H stretching in hidroxyl functional group
2926.11	Asymetric C-H in metil and methylene functional group
2854.74	Simetric C-H in metil and methylene functional group
1745.64	C=O in ester groups in hemicellulose and lignin
1627.97	C=C or C=N from the aromatic region
1437.02	C=C stretching from aromatic region
1375.29	C-H stretching of cellulose
1242.20	C-O-H deformation and C-O stretching in phenolic functional group
1155.40	C-O-C in cellulose dan hemicellulose
1089.82	C-O stretching in cellulose dan hemicellulose
871.85	C-H rocking in cellulose

4.2. Adsorption characteristics of carbon microparticles based on isotherm models

Figure 5 shows the percent adsorption efficiency of carbon microparticles against time. Based on Figure 5, the adsorption efficiency of the carbon microparticle adsorbents having sizes 500, 250, and 100 µm were 34.10, 49.70, and 53.44%, respectively. The adsorption results show that the ability of the adsorbent to absorb adsorbate molecules depends on the particle size. Adsorbents with small particle sizes have the best adsorption efficiency than larger adsorbent particle sizes due to small particles having a high surface area. This is also reinforced by the results of the BET analysis that shows that the small particle size has an impact on the high surface area (see Table 9). In adsorption, smaller particles have a higher specific surface area and more adsorption sites, which may explain why carbon microparticles with an outer diameter of 100 µm have a higher adsorption efficiency to adsorb dye waste compared to sizes 500 and 250 µm. This is consistent with previous findings that adsorbents with small particle sizes have a larger surface area and thus a higher absorption rate (Nandiyanto, Ragadhita & Istadi, 2020).

To investigate the adsorption model, experimental data were subjected to get regression analysis to fit the linearized expression of mathematical models. The experimental values are reconstituted based on the plotting of some parameters (using plot equations in Table 11). Figures 6(a-j) plot analysis results of ten model isotherm adsorptions. The following sections provide detailed explanations for each model.

Figure 6(a) shows the plotting curve of the Langmuir model based on equations 1 and 2. The R^2 value of this model is highest compared to the other model, informing that the adsorption process follows this model. Langmuir's model assumes that the adsorption process is forming a monolayer on a homogeneous adsorbent surface. Based on the Langmuir model, the maximum adsorption capacity (Q_{max}) of carbon par-particles as an adsorbent for sizes 500, 250, and 100 mm is 13.14, 20.45, and 38.76 mg/g, respectively (see Table 11). The separator factor value revealed values ranging from 0 to 1 (see Table 11), indicating that the adsorption process is favorable. The Langmuir adsorption constant (K_L) indicates the degree of adsorbate-adsorbent interaction. A higher K_L value indicates a strong adsorbate-adsorbent interaction, whereas a lower K_L value indicates a weak interaction between the adsorbate molecule and the adsorbent surface. The K_L value for all adsorption systems is relatively small, indicating a weak interaction between the adsorbent and adsorbate molecules due to the active site only adsorbing one molecule.

Figure 6(b) shows the plotting curve of the Freundlich model based on Equation 3. The R^2 in the Freundlich model is greater than 0.80, thus the adsorption process fits with the Freundlich model. Freundlich's model assumes that there is multilayer formation in the adsorbent surface. Analysis of the n and $1/n$ values show that $n < 1$ and $1/n > 1$ informing adsorption profile has chemisorption characteristics with cooperative interaction between adsorbed molecules (see Table 11).

Figure 6(c) is the plotting data based on Temkin isotherm using Equation 5. The adsorption process does not follow the Temkin model due to R^2 being less than 0.80 except adsorption system using small particle size due to $R^2 > 0.80$. Based on the Temkin model, the adsorption process has a physisorption character due to $\beta_T < 8$ kJ/mol (see Table 11). Therefore, based on the Temkin model, the adsorption system using small particle adsorbent shows physisorption characteristics. However, The Temkin equilibrium constant corresponds to the maximum binding energy, and a high A_T indicates an attractive interaction between the adsorbate-adsorbent system. Here, the A_T value for all adsorption systems

is relatively small, indicating that there is less affinity between the adsorbent and adsorbate molecules due to physical interactions, as confirmed by the β_T parameter.

Figure 6(d) shows the Dubinin-Radushkevich isotherm plotting based on Equations 6 and 7. The R^2 is relatively high (R^2 > 0.80), thus adsorption process follows micropore filling. Parameter *E* (see Table 11) in this isotherm describes the interactions between adsorbed molecules with physisorption characteristics. In Table 11, the β parameter is the Dubinin-Radushkevich isotherm constant-related saturation capacity. A high value of the β parameter indicates a high adsorption capacity. Pore volume affects the β value. The greater the pore volume impact the greater the maximum binding energy value.

Figure 6(e) shows Fowler-Guggenheim isotherm plotting based on Equation 8. Based on the analysis, Fowler-Guggenheim has R^2 = 0.0503 which explains the adsorption process does not follow this model. Interaction between adsorbent and adsorbate showed by the K_{FG} value. A higher K_{FG} value indicates a good adsorbent-adsorbate interaction. Because there are surface-active sites that are less efficient in adsorbing the adsorbate molecules due to physical interaction dominance, adsorbent systems show identically small K_{FG} values, indicating weak interaction adsorbent-adsorbate. The interaction energy between the adsorbed molecules (*W*) confirmed repulsive interaction between an adsorbed molecule (*W* < 0 kJ/mol) (see Table 11).

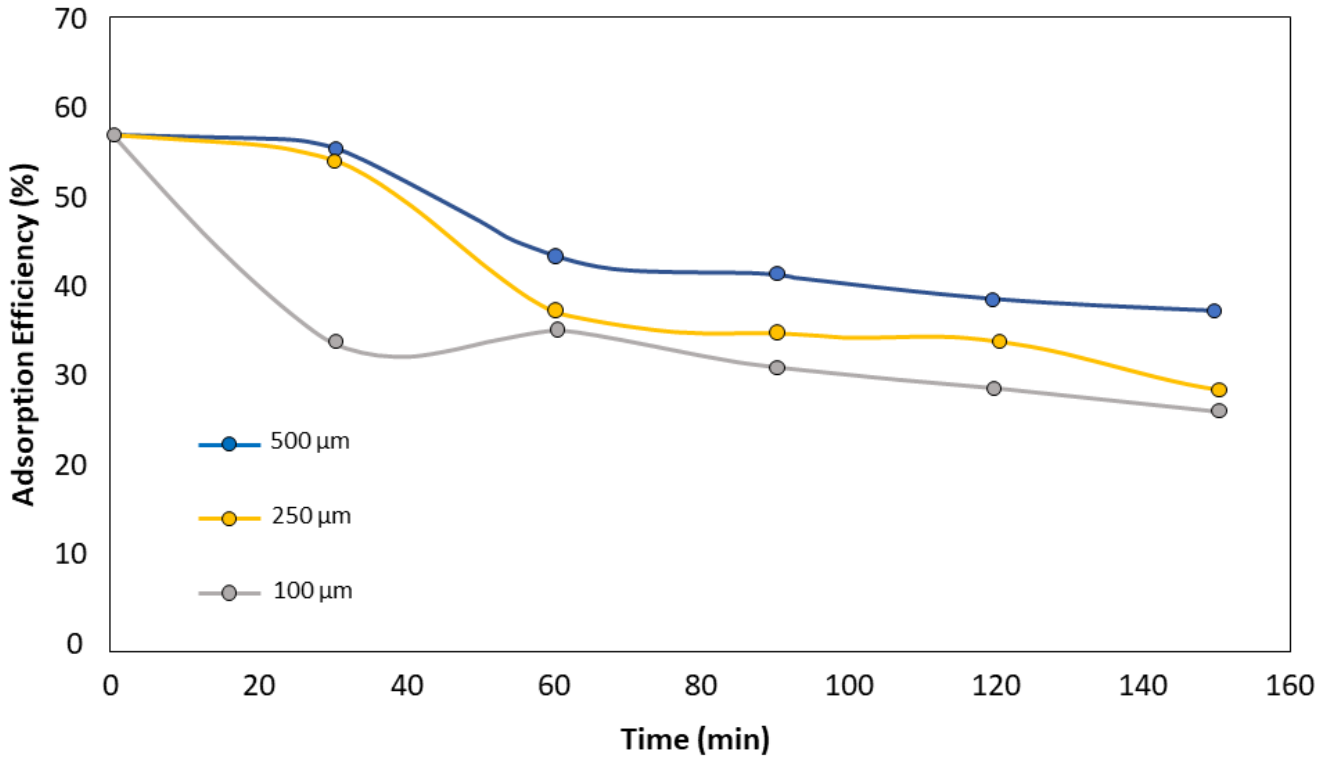

Figure 5. Adsorption efficiency of carbon microparticles against time.

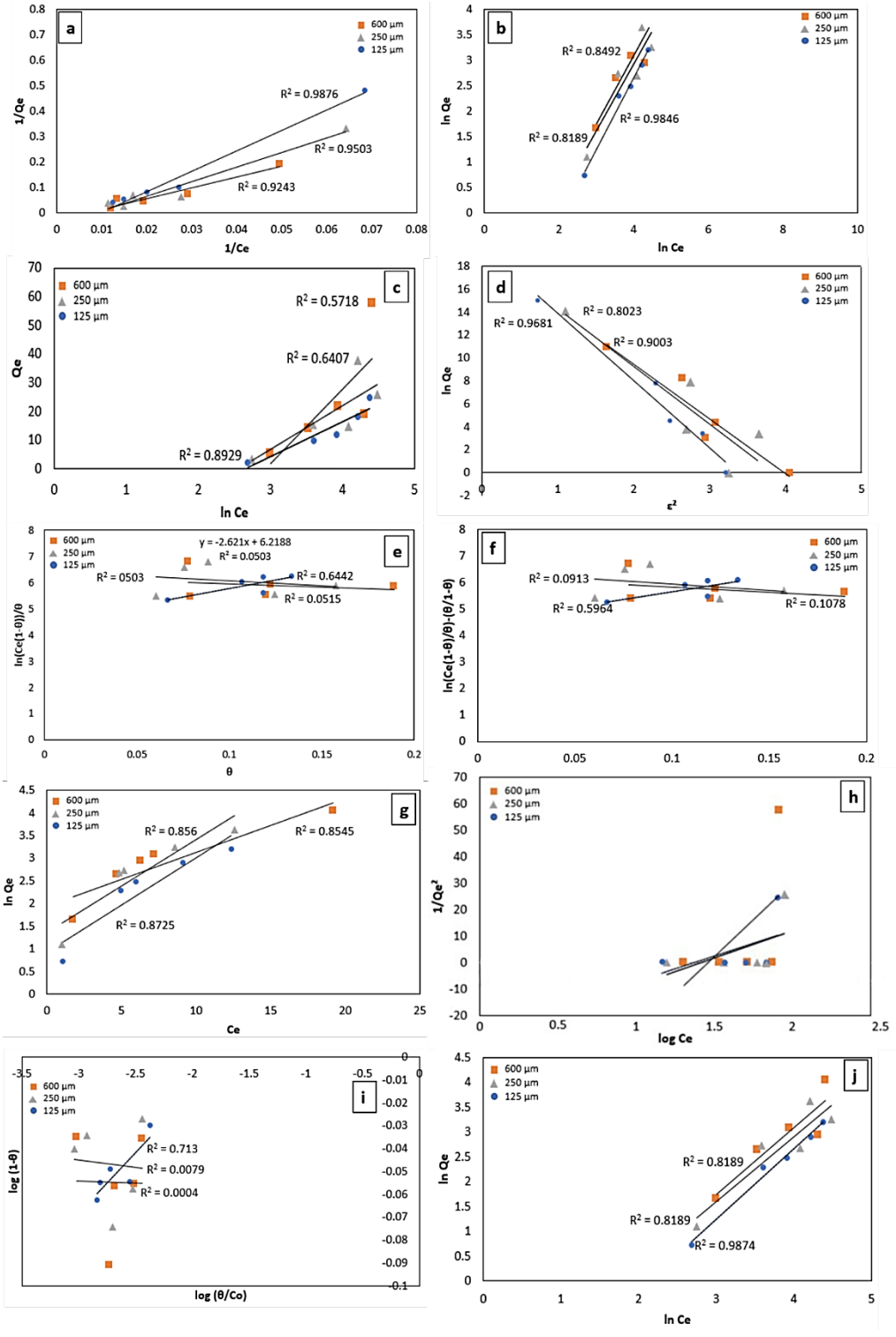

Figure 6. Data fitting with isotherm models Langmuir (a), Freundlich (b), Temkin (c), Dubinin-Radushkevich (d), Fowler-Guggenheim (e), Hill-Deboer (f), Jovanovic (g), Harkin -Jura (h), Flory-Huggins (i), and Halsey (j)

Table 11. Detailed data of adsorption isotherm parameters.

Model	Parameters	Particle Size (μm)			Notes
		100	250	500	
Langmuir	R^2	0.9243	0.9503	0.9876	Monolayer existence on the surface of the adsorbent (R^2 > 0.80)
	Q_{max} (mg/g)	38.759	20.45	13.14	Maximum capacity adsorption
	K_L (L/mg)	0.006	0.008	0.009	The small value Langmuir constant indicates weak interaction between adsorbate and adsorbent
	R_L	0.675-0.892	0.900-0.990	0.894-0.990	Favorable adsorption (0 < R_L <1)
Freundlich	R^2	0.8189	0.8492	0.9846	Multilayer existence on the heterogeneous surface of adsorbent (R^2 > 0.80)
	N	0.743	0.7675	0.7055	Chemisorption (n < 1)
	$1/n$	1.346	1.3028	1.4173	Cooperative adsorption with favorable characteristics ($1/n$ > 1)
	K_f (mg/g)	0.049	0.100	3.842	The adsorption capacity of the adsorbent
Temkin	R^2	0.5718	0.6407	0.8929	Homogenous distribution adsorbate in the adsorbent surface (R^2 < 0.80)
	A_T (L/g)	2.423	0.070	0.071	Temkin equilibrium binding constant
	β_T (J/mol)	86.872	161.731	205.860	Physisorption (β_T < 8 kJ/mol)
Dubinin-Radushkevich	R^2	0.9003	0.8023	0.9681	The adsorbent surface contains micropores (R^2 > 0.80)
	β_T (mol^2/kJ^2)	4.7507	5.0048	5.8589	Dubinin-Radushkevich isotherm constant
	E (kJ/mol)	0.324	0.316	0.292	Physisorption (E < 8 kJ/mol)
Fowler-Guggenheim	R^2	0.0503	0.0515	0.6442	Monolayer existence on the surface of the adsorbent (R^2 < 0.80)
	W (kJ/mol)	-23.795	-27.253	-29.002	Repulsive interaction between an adsorbed molecule (W < 0 kJ/mol)
	K_{FG} (L/mg)	0.002	0.002	0.001	Fowler-Guggenheim isotherm constant
Hill-Deboer	R^2	0.1078	0.0913	0.5964	Monolayer existence on the surface of the adsorbent (R^2 < 0.80)
	K_1 (L/mg)	0.002	0.001	0.010	Hill-Deboer isotherm constant
	K_2 (kJ/mol)	-35.904	-37.056	-39.876	Repulsive interaction between adsorbed molecule (K_2 < 0 kJ/mol)

Jovanovic	R^2	0.8545	0.8725	0.856	Monolayer existence on the surface of the adsorbent (R^2 > 0.80)
	K_J (L/mg)	0.1194	0.2092	0.205	Jovanovic isotherm constant
	Q_{max} (mg/g)	2.522	3.896	6.935	Maximum uptake of adsorbate
Harkin-Jura	R^2	0.3016	0.2882	0.2605	Monolayer existence on the surface of the adsorbent (R^2 < 0.80)
	A_{HJ}	0.017	0.048	0.051	Harkin-Jura isotherm constant
	B_{HJ}	1.392	1.408	1.349	Related to the surface area of the adsorbent
Flory-Huggins	R^2	0.0004	0.0079	0.713	Monolayer existence on the surface of the adsorbent (R^2 < 0.80)
	n_{FH}	0.0021	0.0066	0.0648	The adsorbate occupies more than one active adsorbent zone (n_{FH}< 1)
	K_{FH} (L/mg)	0.870	0.861	1.230	Flory-Huggins isotherm constant
	$\Delta G°$ (kJ/mol)	-0.316	-0.370	-0.512	Spontaneous adsorption ($\Delta G°$ < 0)
Halsey	R^2	0.8189	0.8492	0.9874	No monolayer existence on the surface of the adsorbent (R^2 > 0.80)
	N	0.742	0.767	0.705	Halsey isotherm constant
	K_H	0.181	0.050	0.014	Halsey isotherm constant

The adsorption analysis revealed that the Langmuir isotherm model is the best based on the R^2 value (closer to 1) from linear fitting analysis (see Table 11). According to the data in Table 1, the five best-fit isotherm models are Langmuir > Dubinin-Radushkevich > Jovanovic > Freundlich > Halsey. The five best models are taken because they have an R^2 > 0.80.

Based on the results of the adsorption isotherm analysis, the adsorption system with carbon particle adsorbent from date palm seeds showed adsorption with the formation of monolayer and multilayer. The formation of the monolayer was confirmed by the Langmuir and Jovanovic isotherms. The formation of this monolayer occurs because there are several sites on the adsorbent whose surface is homogeneous. Based on the Langmuir isotherm, adsorption was normal and favorable which was confirmed by the value of the R_L parameter which was between 0 and 1. Meanwhile, Freundlich and Halsey's isotherm model confirmed the existence of multilayer formation on heterogeneous adsorbent surfaces. The values of n <1 and $1/n$ > 1 in the Freundlich model indicate the degree of linearization between adsorbate and adsorbent; the values show that adsorption follows cooperative adsorption with chemical interactions (Ragadhita & Nandiyanto, 2021). Cooperative adsorption provides information about the occurrence of chemical and physical interactions at the same

time (Liu, 2015). The chemical interaction in the adsorption system is consistent with the Temkin model parameter value $\beta_T > 8$ J/mol. The presence of a heterogeneous structure in the adsorbent is also assumed by the Dubinin-Radushkevich isotherm which also contributes to the multilayer adsorption process (Dada et al., 2012). Furthermore, because the parameter value $E < 8$ kJ/mol in the Dubinin-Radushkevich isotherm, the Dubinin-Radushkevich model confirmed the physical interaction. The prediction model for carbon-based adsorbent from date palm seed is illustrated in Figure 7. In addition, since the pores are in the range of micropore size range (about 1.6 nm; see Table 9), we can conclude that all adsorption will be done on the outer surface. Molecules must be less than 1 nm to get the deepest pore position.

5. Conclusion

Isotherm adsorption of carbon particles from date palm seed in an aqueous solution has been successfully investigated. The adsorption process followed suitability with five isotherms, namely Langmuir > Dubinin-Radushkevich > Jovanovic > Freundlich > Halsey. Overall, the adsorption process revealed the formation of monolayers and multilayers on a homogeneous (uniform) surface. The adsorption proceeds normal, spontaneous, and favorable process, with physical and chemical interactions between adsorbate molecules at one time (cooperative adsorption). Adsorption with physisorption interaction has been done for attracting adsorbate molecules to the adsorption site via the Van der Waals force. Meanwhile, there are also molecular interactions where the molecules are attached to the surface through the formation of chemical bonds.

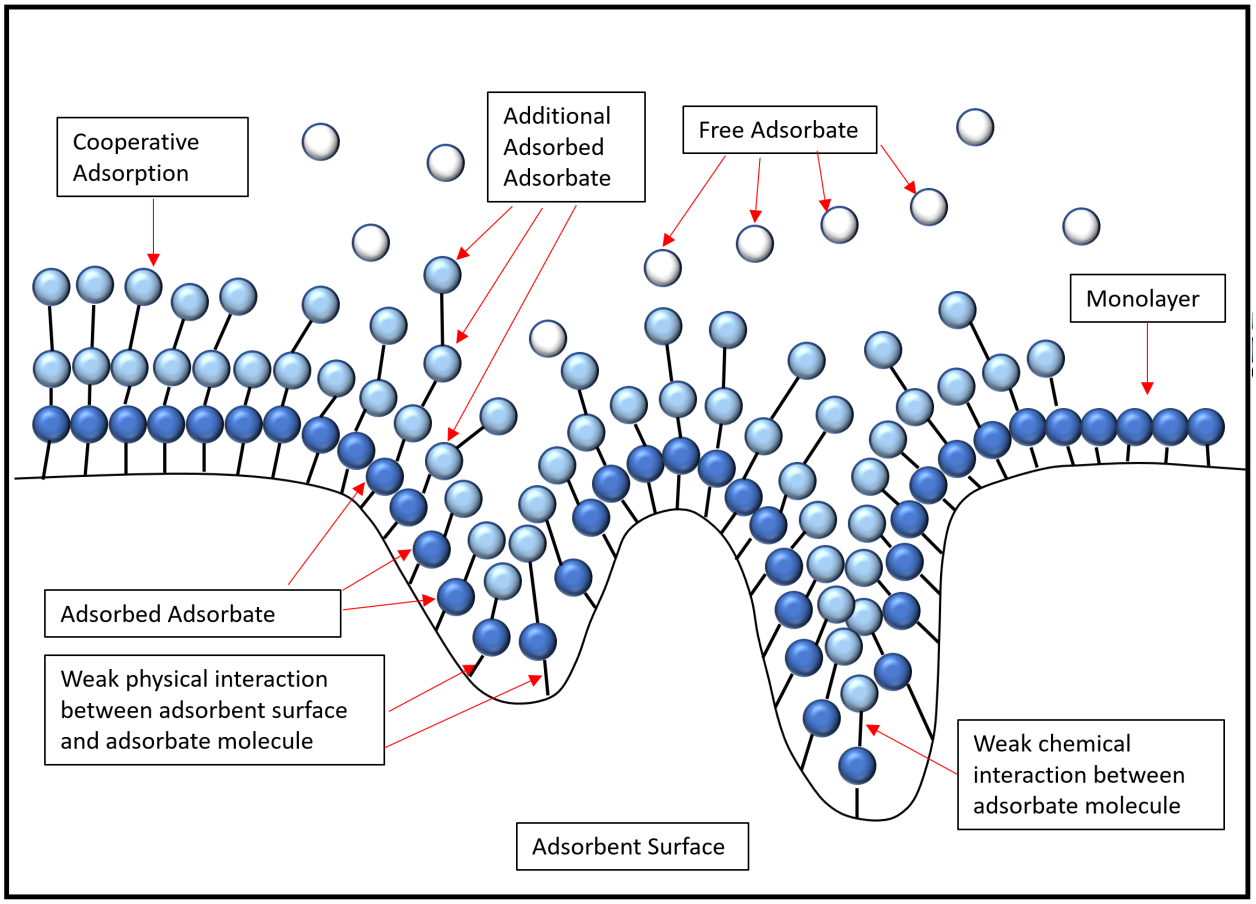

Figure 7. Prediction model for carbon-based adsorbent from date palm seed (adopted from Ragadhita & Nandiyanto, 2021).

Conflict of interest

The authors have no conflict of interest to declare.

Acknowledgments

We thank team members in Nandiyanto Research Group in Univeristas Pendidikan Indonesia for supporting this study.

Funding

We acknowledged Bangdos Universitas Pendidikan Indonesia

References

Anshar, A. M., Taba, P., & Raya, I. (2016). Kinetic and thermodynamics studies the adsorption of phenol on activated carbon from rice husk activated by ZnCl2. *Indonesian Journal of Science and Technology*, *1*(1), 47-60. https://doi.org/10.17509/ijost.v1i1.2213

Awan, M. M. S., Soroushian, P., Ali, A., & Awan, M. Y. S. (2017a High-performance cementitious matrix using carbon nanofibers. *Indonesian Journal of Science and Technology*, *2*(1), 57-75. https://doi.org/10.17509/ijost.v2i1.5989

Awan, M. M. S., Soroushian, P., Ali, A., & Awan, M. Y. S. (2017b). Use of carbon nano-fibers in cementitious mortar. *Indonesian Journal of Science and Technology*, *2*(2), 134-151. https://doi.org/10.17509/ijost.v2i2.8001

Awan, M. S., Ali, A., Perviz, S., & Awan, Y. S. (2019). Car Bouchelta on nano fibre reinforcements in concrete. *Indonesian Journal of Science and Technology*, *4*(1), 1-16. https://doi.org/10.17509/ijost.v4i1.4140

Bouchelta, C., Medjram, M. S., Bertrand, O., & Bellat, J. P. (2008). Preparation and characterization of activated carbon from date stones by physical activation with steam. *Journal of Analytical and Applied Pyrolysis*, *82*(1), 70-77. https://doi.org/10.1016/j.jaap.2007.12.009

Chang, Y. S., Au, P. I., Mubarak, N. M., Khalid, M., Jagadish, P., Walvekar, R., & Abdullah, E. C. (2020). Adsorption of Cu (II) and Ni (II) ions from wastewater onto bentonite and bentonite/GO composite. *Environmental Science and Pollution Research*, *27*, 33270-33296. https://doi.org/10.1007/s11356-020-09423-7

Dada, A. O., Olalekan, A. P., Olatunya, A. M., & Dada, O. J. I. J. C. (2012). Langmuir, Freundlich, Temkin and Dubinin–Radushkevich isotherms studies of equilibrium sorption of Zn2+ unto phosphoric acid modified rice husk. IOSR Journal of applied chemistry, 3(1), 38-45.

Efiyanti, L., Indrawan, D. A., Arif, Z., Hutapea, D., & Septina, A. D. (2020). Synthesis and Application of a Sulfonated Carbon Catalyst for a Hydrolisis Reaction. *Indonesian Journal of Science and Technology*, *5*(3), 410-420. https://doi.org/10.17509/ijost.v5i3.25275

Fiandini, M., Ragadhita, R. I. S. T. I., Nandiyanto, A. B. D., & Nugraha, W. C. (2020). Adsorption characteristics of submicron porous carbon particles prepared from rice husk. Journal of Engineering Science and Technology, 15(1), 022-31.

Jeyavishnu, K., & Alagesan, V. (2020). Cereus sp. as potential biosorbent for removal of Congo red from aqueous solution: isotherm and kinetic investigations. *Environmental monitoring and assessment*, 192, 1-15. https://doi.org/10.1007/s10661-020-8197-2

Liu, S. (2015). Cooperative adsorption on solid surfaces. *Journal of Colloid and Interface Science*, 450, 224-238. https://doi.org/10.1016/j.jcis.2015.03.013

Nabili, A., Fattoum, A., Passas, R., & Elaloui, E. (2016). Extraction and characterization of cellulose from date palm seeds (Phoenix dactylifera L.). Cellul. Chem. Technol, 50, 1015-1023.

Nandiyanto, A. B. D., Girsang, G. C. S., Maryanti, R., Ragadhita, R., Anggraeni, S., Fauzi, F. M., ... & Al-Obaidi, A. S. M. (2020). Isotherm adsorption characteristics of carbon microparticles prepared from pineapple peel waste. *Communications in Science and Technology*, *5*(1), 31-39. https://doi.org/10.21924/cst.5.1.2020.176

Nandiyanto, A. B. D. (2020). Isotherm adsorption of carbon microparticles prepared from pumpkin (Cucurbita maxima) seeds using two-parameter monolayer adsorption models and equations. *Moroccan Journal of Chemistry*, *8*(3), 8-3. https://doi.org/10.48317/IMIST.PRSM/morjchem-v8i3.21636

Nandiyanto, A. B. D., Arinalhaq, Z. F., Rahmadianti, S., Dewi, M. W., Rizky, Y. P. C., Maulidina, A., ... & Yunas, J. (2020). Curcumin Adsorption on Carbon Microparticles: Synthesis from Soursop (AnnonaMuricata L.) Peel Waste, Adsorption Isotherms and Thermodynamic and Adsorption Mechanism. International Journal of Nanoelectronics & Materials, 13. 172-192.

Nandiyanto, A. B. D., Maryanti, R., Fiandini, M., Ragadhita, R., Usdiyana, D., Anggraeni, S., ... & Al-Obaidi, A. S. M. (2020). Synthesis of carbon microparticles from red dragon fruit (Hylocereus undatus) peel waste and their adsorption isotherm characteristics. *Molekul*, *15*(3), 199-209. http://dx.doi.org/10.20884/1.jm.2020.15.3.657

Nandiyanto, A. B. D., Ragadhita, R., & Istadi, I. (2020). Techno-economic analysis for the production of silica particles from agricultural wastes. *Moroccan Journal of Chemistry*, *8*(4), 8-4. https://doi.org/10.48317/IMIST.PRSM/morjchem-v8i4.21637

Nandiyanto, A. B. D., Hofifah, S. N., Inayah, H. T., Putri, S. R., Apriliani, S. S., Anggraeni, S., ... & Rahmat, A. (2021). Adsorption isotherm of carbon microparticles prepared from pumpkin (Cucurbita maxima) seeds for dye removal. *Iraqi Journal of Science*, 1404-1414. https://doi.org/10.24996/ijs.2021.62.5.2

Nandiyanto, A. B. D., Fiandini, M., Ragadhita, R., & Aziz, M. (2023). How to Purify and Experiment with Dye Adsorption using Carbon: Step-by-Step Procedure from Carbon Conversion from Agricultural Biomass to Concentration Measurement Using UV Vis Spectroscopy. *Indonesian Journal of Science and Technology*, *8*(3), 363-380. https://doi.org/10.17509/ijost.v8i3.58290

Nayl, A. E. A., Elkhashab, R. A., El Malah, T., Yakout, S. M., El-Khateeb, M. A., Ali, M. M., & Ali, H. M. (2017). Adsorption studies on the removal of COD and BOD from treated sewage using activated carbon prepared from date palm waste. *Environmental Science and Pollution Research*, *24*, 22284-22293. https://doi.org/10.1007/s11356-017-9878-4

N'diaye, A. D. (2023). Nonlinear Analysis of The Kinetics and Equilibrium for Adsorptive Removal of Paranitrophenol by Powdered Activated Carbon. *ASEAN Journal of Science and Engineering*, *3*(3), 271-280. https://doi.org/10.17509/ajse.v3i3.49136

Ragadhita, R., & Nandiyanto, A. B. D. (2021). How to calculate adsorption isotherms of particles using two-parameter monolayer adsorption models and equations. *Indonesian Journal of Science and Technology*, *6*(1), 205-234. https://doi.org/10.17509/ijost.v6i1.32354

Ragadhita, R., Nandiyanto, A.B.D., Nugraha, W.C., & Mudzakir, A. (2019). Adsorption isotherm of mesopore-free submicron silica particles from rice husk. Journal of Engineering Science and Technology, 14(4), 2052-2062.

Rajabi, M., Keihankhadiv, S., Suhas, Tyagi, I., Karri, R. R., Chaudhary, M., & Singh, P. (2023). Comparison and interpretation of isotherm models for the adsorption of dyes, proteins, antibiotics, pesticides and heavy metal ions on different nanomaterials and non-nano materials—a comprehensive review. *Journal of Nanostructure in Chemistry*, *13*(1), 43-65. https://doi.org/10.1007/s40097-022-00509-x

Sambudi, N. S., Sithambaran, Y., Hui, K. C., Nugraha, M. W., Kamal, N. A., Harun, N. Y., & Sufian, S. Modification of Kaolin with Carbon Quantum Dots as Composite for Methylene Blue Removal: Literature Review and Experiment. *Indonesian Journal of Science and Technology*, *7*(2), 311-336. https://doi.org/10.17509/ijost.v7i2.50810